arXiv:cond-mat/0610547v1 [cond-mat.stat-mech] 19 Oct 2006

Master equation approach to DNA-breathing in heteropolymer DNA

Tobias Ambjörnsson,[1,2,*] Suman K. Banik,[3] Michael A. Lomholt,[1,4] and Ralf Metzler[1,4,†]

[1] *NORDITA (Nordic Institute for Theoretical Physics), Blegdamsvej 17, DK-2100 Copenhagen Ø, Denmark.*

[2] *Present address: Department of Chemistry, Massachusetts Institute of Technology, 77 Massachusetts Avenue, Cambridge, MA 02139, USA*

[3] *Dept. of Physics, Virginia Polytechnic Institute and State University, Blacksburg, VA 24061-0435, USA*

[4] *Present address: Department of Physics, University of Ottawa, 150 Louis Pasteur, Ottawa, Ontario K1N 6N5, Canada*

After crossing an initial barrier to break the first base-pair (bp) in double-stranded DNA, the disruption of further bps is characterized by free energies between less than one to a few k_BT. This causes the opening of intermittent single-stranded bubbles. Their unzipping and zipping dynamics can be monitored by single molecule fluorescence or NMR methods. We here establish a dynamic description of this DNA-breathing in a heteropolymer DNA in terms of a master equation that governs the time evolution of the joint probability distribution for the bubble size and position along the sequence. The transfer coefficients are based on the Poland-Scheraga free energy model. We derive the autocorrelation function for the bubble dynamics and the associated relaxation time spectrum. In particular, we show how one can obtain the probability densities of individual bubble lifetimes and of the waiting times between successive bubble events from the master equation. A comparison to results of a stochastic Gillespie simulation shows excellent agreement.

PACS numbers: 05.40.-a,82.37.-j,87.15.-v,02.50.-r

I. INTRODUCTION

Even at room temperature the DNA double-helix opens up locally to form intermittent flexible single-stranded domains, the *DNA-bubbles*. Their size increases from a few broken base-pairs (bps) to a few hundred open bps just below the melting temperature T_m, until a transition occurs to full denaturation [1, 2, 3, 4]. DNA stability is effected by combination of the free energies $\epsilon_{\rm hb}$ for breaking a Watson-Crick hydrogen bond between complementary AT and GC bases in a single bp, and the ten independent stacking free energies $\epsilon_{\rm st}$ for disrupting the interactions between a nearest neighbor pair of bps. At 100 mM NaCl concentration and $T = 37°$C the hydrogen bonding amounts to $\epsilon_{\rm hb} = 1.0k_BT$ for a single AT and $0.2k_BT$ for a GC-bond [5]. The weakest (strongest) stacking energies was found to be the TA/AT (GC/CG) with free energies $\epsilon_{\rm st} = -0.9k_BT$ ($-4.1k_BT$). Note that negative values for the free energies denote stable states. The relatively small free energies for base stacking stem from the fact that relatively large amounts of binding enthalpy on the one hand, and entropy release on breaking the stacking interactions and Watson-Crick bonds on the other hand, almost cancel. Bubble initiation, in contrast, is characterized by breaking of two stacking interactions with the first bp, whose enthalpy cost cannot be balanced by the two, still strongly confined, liberated bases. Thus, the creation of two boundaries between the intact double-helix and the bubble nucleus is associated with an activation cost of some 7 to 12 k_BT corresponding to the Boltzmann factor $\sigma_0 \simeq 10^{-3} \ldots 10^{-5}$ [2, 3, 6, 7]. The cooperativity parameter σ_0 is related to the ring-factor ξ used in [8, 9], see below. The high bubble initiation barrier indeed guarantees the stability of DNA at physiological conditions. Bubble opening occurs predominantly in zones rich in the weaker AT bps; with increasing T, they spread to regions with progressively higher GC content [1, 2, 3]. Thermally driven, a DNA-bubble fluctuates in size by relative random motion of the two zipper forks. In addition to observations using NMR techniques [10], this *DNA-breathing* was recently monitored on the single bubble level by fluorescence correlation methods, demonstrating a multistate kinetics that reflects the stepwise unzipping and zipping of bps. The lifetime of a bubble was shown to range up to a few ms [11].

From a biology or biochemistry point of view, DNA-breathing is of interest, as it is implicated to influence the binding of binding proteins, enzymes, and other chemicals to DNA. Thus, the relatively fast bubble dynamics with respect to the binding rates of proteins, that selectively bind to single-stranded DNA, provides a kinetic block preventing DNA denaturation through these proteins [12, 13, 14]. This was investigated in detail on the bases of a homopolymer approach in Refs. [15, 16]. Similarly, the increase of the bubble formation probability as well as of the bubble lifetime at certain places along the sequence is believed to facilitate the initiation of transcription by RNA polymerase. This latter point is studied in depth in Ref. [17].

In this paper we investigate a $(2 + 1)$-variable master equation, that governs the time evolution of the probability distribution $P(m, x_L, t)$ to find a bubble consisting of m broken bps with left fork position x_L along the se-

*Electronic address: ambjorn@nordita.dk

†Electronic address: metz@nordita.dk

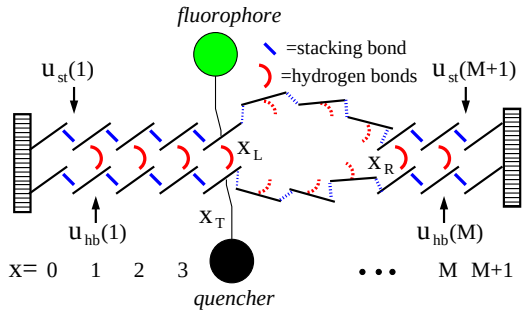


FIG. 1: Clamped DNA domain with internal bps $x = 1$ to M, statistical weights $u_{\rm hb}(x)$, $u_{\rm st}(x)$, and tag position x_T. The DNA sequence enters through the statistical weights $u_{\rm st}(x)$ and $u_{\rm hb}(x)$ for disrupting stacking and hydrogen bonds, respectively. The bubble breathing process consists of the initiation of a bubble and the subsequent motion of the forks at positions x_L and x_R, see also Fig. 2.

quence. With this approach, that is, an arbitrary DNA sequence can be analyzed, and its breathing behavior predicted. We discuss the exact form of the transfer matrix containing the rate coefficients for all permitted moves, and derive the bubble autocorrelation function with associated relaxation time spectrum. To be able to connect to the time series obtained from the complementary stochastic simulation, we derive the probability densities according to which individual bubble lifetimes and the time intervals between successive bubble events are distributed. Finally, we show that in the homopolymer limit, analytical results can be obtained.

II. ONE BUBBLE PARTITION FUNCTION AND TRANSFER COEFFICIENTS

Below the melting temperature T_m, a single bubble can be considered to be statistically independent due to the high nucleation barrier for initiating a bubble quantified by $\sigma_0 \ll 1$ [16], such that opening and merging of multiple bubbles are rare, and a one-bubble picture is appropriate. In the particular case of the bubble constructs used in the fluorescence correlation experiments of Ref. [11], the sequence is designed such that there is a single bubble domain. Referring to these constructs, we consider a segment of double-stranded DNA with M internal bps. These bps are clamped at both ends such that the bps $x = 0$ and $x = M + 1$ are always closed (Fig. 1). The sequence of bps determines the Boltzmann weights $u_{\rm hb}(x) = \exp\{\epsilon_{\rm hb}(x)/(k_BT)\}$ for Watson-Crick hydrogen bonding at position x, and the Boltzmann factor $u_{\rm st}(x) = \exp\{\epsilon_{\rm st}(x)/(k_BT)\}$ for pure bp-bp stacking between bps $x-1$ and x, respectively. In the bubble domain, the left and right zipper fork positions x_L and x_R denoting the right- and leftmost closed bp of the bubble are stochastic quantities, whose random motion underlies the bubble dynamics.

Instead of using the fork positions x_L and x_R, we prefer to work with the left fork position x_L and the bubble size $m = x_R - x_L - 1$. For these variables, the partition function of the bubble becomes

$$\mathscr{Z}(x_L, m) = \frac{\xi'}{(1+m)^c} \prod_{x=x_L+1}^{x_L+m} u_{\rm hb}(x) \prod_{x=x_L+1}^{x_L+m+1} u_{\rm st}(x) \qquad (1)$$

for $m \geq 1$. At $m = 0$, we define $\mathscr{Z}(m = 0) = 1$. In relation (1), instead of the usual cooperativity parameter σ_0 we use the factor $\xi' = 2^c\xi$ related to the ring factor $\xi \approx 10^{-3}$ introduced in Ref. [8]. For a homopolymer, this ξ is related to σ_0 by $\sigma_0 = \xi \exp\{\epsilon_{\rm st}/(k_BT)\}$ [8]. The denominator in Eq. (1) represents the entropy loss on formation of a closed polymer loop, where the offset by one accounts for finite size effects [6, 18]. The associated critical exponent is $c = 1.76$ [19]. For a given bubble size, the partition (1) counts m contributions from broken hydrogen bonds and $m + 1$ from disrupted stacking interactions. The partition (1) defines the equilibrium probability

$$P^{\rm eq}(x_L, m) = \frac{\mathscr{Z}(x_L, m)}{\mathscr{Z}(0) + \sum_{m=1}^{M} \sum_{x_L=0}^{M-m} \mathscr{Z}(x_L, m)} \qquad (2)$$

for finding a bubble of size m at location x_L.

The two variables m and x_L are the slow variables of the breathing dynamics, while the polymeric degrees of freedom of the relatively small bubble enter effectively through the partition (1). We moreover assume that the bubble is always close to thermal equilibrium such that the partition (1) defines the transition probabilities between different states. These conditions allow us to introduce the master equation (9) with its transfer matrix $\mathscr{W}$ below. To introduce the underlying time scales, we first define the transfer coefficients.

The allowed transitions with the associated transfer (rate) coefficients are sketched in Fig. 2. The left zipper fork is characterized by the rate $\mathsf{t}_L^+(x_L, m)$ corresponding to the process $x_L \to x_L + 1$ of bubble size decrease, and $\mathsf{t}_L^-(x_L, m)$ for $x_L \to x_L - 1$ (bubble size increase). Similarly, we introduce $\mathsf{t}_R^+(x_L, m)$ for $x_R \to x_R + 1$ (bubble size increase) and $\mathsf{t}_R^-(x_L, m)$ for $x_R \to x_R - 1$ (decrease). These rates are valid for transitions between states with $m \geq 1$. Bubble opening (initiation) $m = 0 \to m = 1$ is quantified by $\mathsf{t}_G^+(x_L)$, and bubble closing (annihilation) $m = 1 \to 0$ by $\mathsf{t}_G^-(x_L)$. Note that by our definitions $\mathsf{t}_G^+(x_L)$ and $\mathsf{t}_G^-(x_L)$ actually correspond to bubble opening/closing at $x = x_L+1$. Clamping requires that $x_L \geq 0$ and $x_R \leq M + 1$, corresponding to reflecting boundary conditions [21]

$$\mathsf{t}_L^-(x_L = 0, m) = \mathsf{t}_R^+(x_L, m = M - x_L) = 0. \qquad (3)$$

In Fig. 3 we sketch schematically the allowed transitions in the m-x_L plane.

In order to define the various transfer rates t, we firstly impose the detailed balance conditions (compare [20, 22])

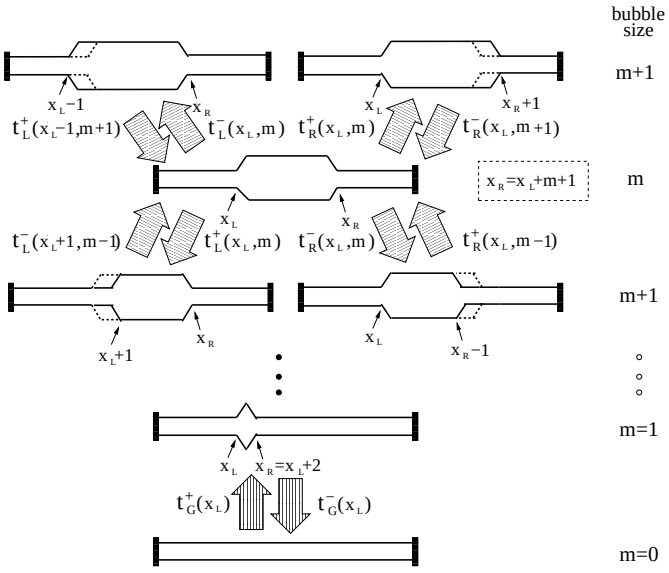


FIG. 2: Possible bubble (un)zipping transitions: for $m \geq 2$, the four transfer rates $\mathsf{t}^{\pm}_{L/R}(x_L, m)$ completely determine the transitions *out of* this state; the coefficients $\mathsf{t}^{\pm}_{L}(x_L \mp 1, m \pm 1)$ and $\mathsf{t}^{\pm}_{R}(x_L, m \mp 1)$ specify the possible jumps *into* this state. Jumps between state $m = 1$ and ground state $m = 0$ are described by $\mathsf{t}^{+}_{G}(x_L)$ and $\mathsf{t}^{-}_{G}(x_L)$.

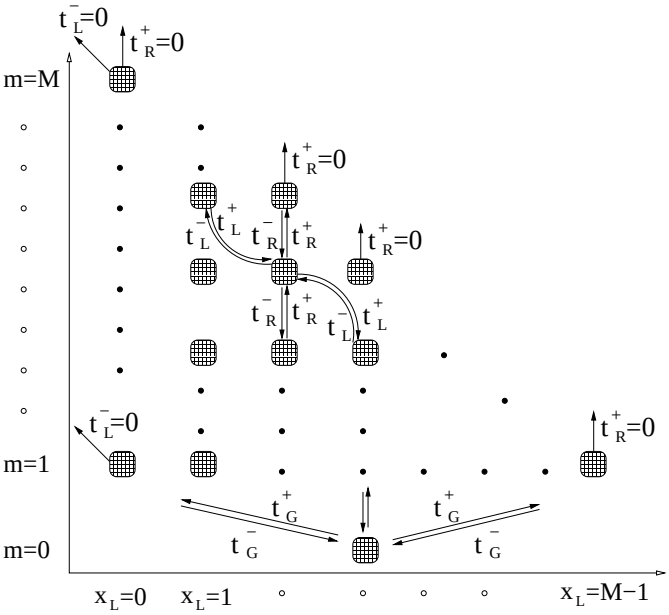


FIG. 3: Schematic representation of the (x_L, m)-lattice on which the DNA-bubble jump process takes place, with the permitted transitions; compare to Figs. 1 and 2. The boundary conditions Eq. (3) are also indicated.

$$\frac{\mathsf{t}^{+}_{L}(x_L - 1, m + 1)}{\mathsf{t}^{-}_{L}(x_L, m)} = \frac{P_{\rm eq}(x_L, m)}{P_{\rm eq}(x_L - 1, m + 1)} \tag{4a}$$

$$\frac{\mathsf{t}^{-}_{R}(x_L, m + 1)}{\mathsf{t}^{+}_{R}(x_L, m)} = \frac{P_{\rm eq}(x_L, m)}{P_{\rm eq}(x_L, m + 1)} \tag{4b}$$

$$\frac{\mathsf{t}^{+}_{G}(x_L)}{\mathsf{t}^{-}_{G}(x_L)} = \frac{P_{\rm eq}(x_L, 1)}{P_{\rm eq}(0)}, \tag{4c}$$

that ensure relaxation toward the equilibrium distribution $P^{\rm eq}(x_L, m)$, see Eq. (2). The latter can be seen by recalling that the equilibrium distribution (2) is based on the Boltzmann factors $u_{\rm hb}$ and $u_{\rm st}$ through the partition (1). The detailed balance conditions do not uniquely define the transfer rates t, leaving a certain freedom of choice [22]. We use the following conventions.

To define the zipping rate, we assume that it is independent of the position x along the DNA sequence. The picture behind is that the closure of the bp is dominated by the requirement that the two bases diffuse in real space until mutual encounter and eventual bond formation. As sterically AT and GC bps are very similar, the zipping rate should not significantly vary with the individual nature of the involved bps, and we choose the constant rate $k/2$, see below. This rate k is the only adjustable parameter of our model, and has to be independently determined from experiment or more fundamental models. This choice, as mentioned above, is not unique. Instead, an x-dependence of k could easily be introduced by choosing different powers of the statistical weights entering the rate coefficients such that they still fulfill detailed balance.

Decrease in bubble size due to zipping close of the bp closest to either the left or the right zipper fork is therefore ruled by

$$\mathsf{t}^{+}_{L}(x_L, m)|_{m\geq 2} = t^{-}_{R}(x_L, m)|_{m\geq 2} = \frac{k}{2}, \tag{5}$$

respectively. The factor $1/2$ is introduced for consistency with previous approaches [15, 16]. Note that for simplicity we do not introduce the hook exponent discussed in previous studies [16, 17, 24]. This exponent should be important for large bubbles, when during the zipping process not only the bp at the zipper fork is moved, but also part of the vicinal single-strand is dragged or pushed along [16, 24, 25].

Increase in bubble size is controlled by

$$\mathsf{t}^{-}_{L}(x_L, m) = \frac{k}{2} u_{\rm st}(x_L) u_{\rm hb}(x_L) s(m), \tag{6a}$$

$$\mathsf{t}^{+}_{R}(x_L, m) = \frac{k}{2} u_{\rm st}(x_R + 1) u_{\rm hb}(x_R) s(m), \tag{6b}$$

for $m \geq 1$, where

$$s(m) = \left(\frac{1 + m}{2 + m}\right)^{c}. \tag{7}$$

For $m \geq 1$ we thus take the bubble increase rate coefficients proportional to the first power of the Arrhenius factor $u_{\rm st} u_{\rm hb} = \exp\{(\epsilon_{\rm hb} + \epsilon_{\rm st})/[k_B T]\}$ times the loop

correction $s(m)$. We stress that Eqs. (6a) and (6b) are dictated by the detailed balance condition, once the convention (5) is established. As noted, detailed balance would still be fulfilled, for instance, if only a fractional power α^q of the Arrhenius factor α appeared in the opening rates if complemented by the respective power α^{1-q} in the closing rates.

Finally, we define

$$\begin{aligned} \mathsf{t}_G^+(x_L) &= k\xi' s(0) u_{\rm st}(x_L+1) u_{\rm hb}(x_L+1) \\ &\quad \times u_{\rm st}(x_L+2) \qquad (8a) \\ \mathsf{t}_G^-(x_L) &= k \qquad (8b) \end{aligned}$$

for bubble initiation and annihilation from and to the zero-bubble state $m = 0$, with the bubble initiation factor ξ' in the expression for t_G^+. As bubble initiation involves breaking of two stacking interactions at consecutive bps, we have the factor $u_{\rm st}(x_L+1)u_{\rm st}(x_L+2)$ in expression (8a). The last open bp can zip close from either side, so the bubble closing rate $\mathsf{t}_G^-(x_L)$ makes up twice the zipping rate of a single fork.

The rates t together with the boundary conditions fully determine the bubble dynamics. In the next Section, we establish the master equation for the time evolution of the distribution $P(m, x_L, t)$ and derive the associated quantities.

III. MASTER EQUATION FOR DNA-BREATHING

The joint probability distribution $P(t) = P(x_L, m, t; x_L', m', 0)$ measures the likelihood that at time t the system is in state $\{x_L, m\}$ and that at $t = 0$ it was in state $\{x_L', m'\}$. Its time evolution is controlled by the master equation

$$\frac{\partial}{\partial t} P(t) = \mathscr{W} P(t). \qquad (9)$$

The explicit form of the transfer matrix $\mathscr{W}$ is discussed in detail in Sec. IV. Here, we concentrate on how to derive the quantities relevant for the description of DNA-breathing experiments. In that course we introduce the eigenmode ansatz [20, 22]

$$P(t) = \sum_p c_p Q_p \exp(-\eta_p t), \qquad (10)$$

where the coefficients c_p are fixed by the initial condition. Combining Eqs. (10) and (9), the eigenvalue equation

$$\mathscr{W} Q_p = -\eta_p Q_p \qquad (11)$$

yields, compare Ref. [22] and below for more details. The eigenvalues η_p and eigenvectors Q_p allow one to compute any quantity of interest. In fact, the autocorrelation function for bubble breathing and the corresponding relaxation time distribution are quite straightforward to obtain, see section III A. Below, in section III B, we discuss the more subtle point how the probability densities for the bubble lifetime and the interbubble event waiting time can be derived.

A. Blinking autocorrelation function of a tagged bp

Motivated by the fluorescence correlation setup in Ref. [11] we are interested in the state of a tagged bp at $x = x_T$, see Fig. 1. In the experiment fluorescence occurs if the bps in a Δ-neighborhood of the fluorophore position x_T are open [11]. Measured fluorescence blinking time series thus correspond to the stochastic variable $I(t)$, defined by

$$I(t) = \begin{cases} 1 & \text{at least all bps in } [x_T - \Delta, x_T + \Delta] \text{ open} \\ 0 & \text{otherwise,} \end{cases} . \qquad (12)$$

The stochastic variable is $I = 1$ if the system is in the phase space region defined by

$$\mathbb{R}1 : \{0 \leqslant x_L \leqslant x_T - \Delta - 1,\ x_T - x_L + \Delta \leqslant m \leqslant M - x_L\}. \qquad (13)$$

Conversely, $I = 0$ corresponds to the complement $\mathbb{R}0$.

The equilibrium autocorrelation function of fluorescence blinking is defined by

$$A(x_T, t) = \langle I(t) I(0) \rangle - (\langle I \rangle)^2, \qquad (14)$$

where the angles $\langle \cdot \rangle$ denote an ensemble average over the equilibrium distribution $P_{\rm eq}$. $A(x_T, t)$ quantifies the relaxation dynamics of the tagged bp. This is evident from the identity

$$\langle I(t) I(0) \rangle = \sum_{I=0}^{1} \sum_{I'=0}^{1} I \rho(I, t; I', 0) I' = \rho(1, t; 1, 0), \qquad (15)$$

where $\rho(1, t; 1, 0)$ is the survival probability that $I(t) = 1$ and that $I(0) = 1$. From the definition of the two regions $\mathbb{R}1$ and $\mathbb{R}0$ it follows that $\rho(1, t; 1, 0)$ yields from summation of $P(x_L, m, t; x_L', m', 0)$ solely over region $\mathbb{R}1$:

$$\rho(1, t; 1, 0) = \sum_{x_L, m, x_L', m' \in \mathbb{R}1} P(x_L, m, t; x_L', m', 0). \qquad (16)$$

Together with Eq. (15), combined with the eigenmode decomposition (10), and under the assumption that initially the system is at equilibrium, we obtain

$$P(x_L, m, 0; x_L', m', 0) = \delta_{mm'} \delta_{x_L x_L'} P_{\rm eq}(x_L, m), \qquad (17)$$

such that we can rewrite the autocorrelation function (14) in the form

$$A(x_T, t) = \sum_{p \neq 0} \left[T_p(x_T) \right]^2 \exp(-t/\tau_p). \qquad (18)$$

Here, we use the relaxation times $\tau_p = 1/\eta_p$, and abbreviate

$$T_p(x_T) = \sum_{x_L=0}^{x_T-\Delta-1} \sum_{m=x_T-x_L+\Delta}^{M-x_L} Q_p(x_L, m). \quad (19)$$

In all illustrations, we plot the normalized form of the autocorrelation function, $A(x_T,t)/A(x_T,0) = A(x_T,t)/\sum [T_p(x_T)]^2$.

The autocorrelation function $A(x_T,t)$ can be rewritten as the integral $A(x_T,t) = \int d\tau \exp(-t/\tau) f(x_T,\tau)$ defining the weighted spectral density (relaxation time spectrum) density

$$f(x_T,\tau) = \sum_{p\neq 0} [T_p(x_T)]^2 \delta(\tau - \tau_p). \quad (20)$$

This quantity indicates how many different exponential modes contribute to the autocorrelation function. If $f(x_T,\tau)$ is very narrow, the process is approximately exponential, whereas a broad relaxation time spectrum indicates that many different modes play together.

B. Survival and waiting time densities of a tagged bp

The autocorrelation function $A(x_T,t)$ is an equilibrium average measure for a single bubble. It does not contain any information on how the lifetime of individual bubbles is distributed, nor on the waiting time that elapsed between annihilation of a bubble and the initiation of the next. This information is provided by the survival time and waiting time densities $\phi(t)$ and $\psi(t)$. Here we derive these two quantities.

Survival time and the waiting time densities correspond to a first passage problem, to respectively start from an initial state with $I(0) = 1$ or $I(0) = 0$, and transit to a state $I(t) = 0$ or $I(t) = 1$ after time t. To obtain these quantities from the master equation framework, one needs to solve the reduced eigenvalue problem [22]

$$\mathscr{W}\bar{Q}_p = -\bar{\eta}_p \bar{Q}_p \quad (21)$$

for coordinates belonging to $\mathbb{R}1$ and $\mathbb{R}0$. Details are collected in Sec. IV. The reduced eigenvalue ansätze (21) for $\mathbb{R}1$ and $\mathbb{R}0$ possess only positive eigenvalues, $\bar{\eta}_p > 0$ for all p. This reflects the fact that there exist transitions from one region to the other, such that probability "leaks out". In terms of the reduced eigenvalues $\bar{\eta}_p$ and eigenvectors $\bar{Q}_p$ the survival and waiting time densities become

$$\psi(t) = \sum_{p\in\mathbb{R}0} \bar{\eta}_p \bar{c}_p \exp(-\bar{\eta}_p t) \quad (22a)$$

$$\phi(t) = \sum_{p\in\mathbb{R}1} \bar{\eta}_p \bar{c}_p \exp(-\bar{\eta}_p t) \quad (22b)$$

with the coefficients

$$\bar{c}_p = \frac{\bar{\eta}_p [\sum_{x_L,m} \bar{Q}_p(x_L,m)]^2}{\sum_p \bar{\eta}_p [\sum_{x_L,m} \bar{Q}_p(x_L,m)]^2}. \quad (22c)$$

The sums over m, x_L are restricted to regions $\mathbb{R}1$ and $\mathbb{R}0$ for the survival and waiting time densities, respectively. Both survival and waiting time probability densities are normalized, $\int \psi(t)dt = 1$ and $\int \phi(t)dt = 1$, since $\sum_p \bar{c}_p = 1$.

We point out that a non-trivial problem connected to obtaining the appropriate expressions for $\psi(t)$ and $\phi(t)$ is how to choose the right initial distribution of states (there are many states corresponding to a bubble being just open/closed). We chose an initial distribution determined by the distribution of stationary flux into the regions $\mathbb{R}1$ and $\mathbb{R}0$. This choice guarantees that (for long times) the ratio of the time spent in the $I = 1$ state versus the time spent in the $I = 0$ state is given by the equilibrium results as required by ergodicity, see Sec. IV for details. In appendix A we briefly discuss how stochastic modeling can be used to obtain single bubble time series, from which all quantities such as fluorescence blinking autocorrelation function, as well as the survival and waiting time densities can be distilled. Both approaches converge nicely [17, 24].

IV. MASTER EQUATION - THE DETAILS

In this Section we show the explicit form for the master equation with its transfer matrix $\mathscr{W}$ and go into details of how to solve it numerically. We also develop a formalism to derive the waiting and survival densities $\psi(t)$ and $\phi(t)$.

A. The $\mathscr{W}$-matrix

In order to present an explicit expression for the $\mathscr{W}$-matrix in Eqs. (9) and (11) it is convenient to replace the two-dimensional grid points (x_L, m) by a one-dimensional coordinate s counting all lattice points, compare [16]. We choose the enumeration illustrated in figure 4. From this figure we notice that $m \in [0, M]$ and $x_L \in [0, M-m]$. We label the ground state $m = 0$ by $s = 0$. For $m \geq 1$ an arbitrary s-point can be obtained from a specific (x_L, m) according to:

$$s = s|_{x_L}^{m} = (m-1)M - \frac{(m-1)(m-2)}{2} + x_L + 1 \quad (23)$$

From this relation we notice that the maximum s value is

$$S = \max\{s\} = \frac{M(M+1)}{2}, \quad (24)$$

i.e., the size of the relevant $\mathscr{W}$-matrix (see below) scales as M^2. Expression (23) allows us to change the transfer coefficients to the s-variable, $\mathsf{t}^{\pm}_{L/R}(x_L, m) \to \mathsf{t}^{\pm}_{L/R}(s)$,

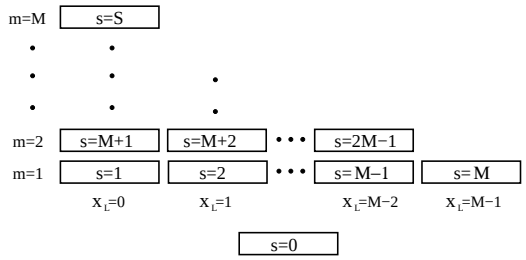


FIG. 4: Enumeration scheme for the numerical analysis: The two-dimensional grid points (x_L, m) are replaced by a one-dimensional running variable s. See text for details.

using the explicit expressions (5), (6a), and (6b) for the transfer coefficients, together with the boundary conditions in Eqs. (3). Also $\mathsf{t}_G^{\pm}(x_L,m) \to \mathsf{t}_G^{\pm}(s)$, following Eqs. (8a) and (8b). From Eq. (23) and figure 4 we notice that

$$\begin{aligned} s|_{x_L-1}^{m+1} &= s|_{x_L}^{m} + M - m, \text{ for } x_L \geq 1 \;\&\; m \leq M-1, \\ s|_{x_L+1}^{m-1} &= s|_{x_L}^{m} - (M-m+1), \text{ for } m \geq 2, \\ s|_{x_L}^{m-1} &= s|_{x_L}^{m} - (M-m+2), \text{ for } m \geq 2, \\ s|_{x_L}^{m+1} &= s|_{x_L}^{m} + M - m + 1, \\ &\quad \text{for } x_L \leq M-(m+1) \;\&\; m \leq M-1. \end{aligned} \tag{25}$$

We can then write Eq. (11) explicitly as

$$\sum_{s'} \mathscr{W}(s,s')Q_p(s') = -\eta_p Q_p(s), \tag{26}$$

where the matrix-elements are

$$\begin{aligned} \mathscr{W}(s, s+M-m) &= \mathsf{t}_L^+(s+M-m), \\ &\quad \text{for } s \Cap x_L \geq 1 \,\&\, m > 1 \\ \mathscr{W}(s, s-[M-m+1]) &= \mathsf{t}_L^-(s-[M-m+1]), \\ &\quad \text{for } s \Cap m \geq 2 \\ \mathscr{W}(s, s-[M-m+2]) &= \mathsf{t}_R^+(s-[M-m+2]), \\ &\quad \text{for } s \Cap m \geq 2, \\ \mathscr{W}(s, s+M-m+1) &= \mathsf{t}_R^-(s+M-m+1), \\ &\quad \text{for } s \Cap x_L \leq M-(m+1) \\ &\quad \& \; 1 \leq m \leq M-1, \\ \mathscr{W}(s,s) &= -(\mathsf{t}_L^+(s) + \mathsf{t}_L^-(s) \\ &\quad + \mathsf{t}_R^+(s) + \mathsf{t}_R^-(s)), \\ &\quad \text{for } s \Cap m \geq 2. \end{aligned} \tag{27}$$

We have introduced the notation $s \Cap$ with the meaning "s is to be taken for". The positive terms above correspond to jumps *to* the state $\{x_L, m\}$, while the negative terms correspond to jumps *from* the state $\{x_L, m\}$, see Figs. 2 and 3. The probability for a bubble of size $m = 1$ is altered by exchange with the $m = 2$ state, or the $m = 0$ ground state:

$$\begin{aligned} \mathscr{W}(0, x_L+1) &= \mathsf{t}_G^+(x_L), \text{for } s \Cap m = 1, \\ \mathscr{W}(s,s) &= -(\mathsf{t}_G^-(x_L) + \mathsf{t}_L^-(s) + \mathsf{t}_R^+(s)), \\ &\quad \text{for } s \Cap m = 1. \end{aligned} \tag{28}$$

Finally, for the ground state population, we find

$$\begin{aligned} \mathscr{W}(0, x_L+1) &= t_G^-(x_L), \text{ for } x_L \leq M-1 \\ \mathscr{W}(0,0) &= -\sum_{x_L=0}^{M-1} t_G^+(x_L), \end{aligned} \tag{29}$$

i.e., the $m = 0$ state can change by jumping to this state from $m = 1$ (first term) or by jumping out of the $m = 0$ state (second term). There are M possible jumps out from or to the ground state, corresponding to bubble opening or closing at any of the M internal bps. The remaining matrix elements are equal to zero. The problem at hand is that of determining the eigenvalues and eigenvectors of the $(S+1)\times(S+1)$-matrix $\mathscr{W}$ above. In terms of the running variable s, see Eq. (23), and the $\mathscr{W}$-matrix defined in Eqs. (27), (28) and (29) the detailed balance conditions (4) can be written as

$$\mathscr{W}(s,s')P_{\rm eq}(s') = \mathscr{W}(s',s)P_{\rm eq}(s). \tag{30}$$

The eigenvectors are orthonormal in the sense [22]

$$\sum_s \frac{Q_p(s)Q_{p'}(s)}{P^{\rm eq}(s)} = \delta_{p,p'}. \tag{31}$$

Convenient checks of the numerical results then include: (i) there should be one zero eigenvalue $\eta_0 = 0$, the corresponding eigenvector is the equilibrium distribution, i.e. $Q_0(s) = P^{\rm eq}(s)$; (ii) the remaining eigenvalues should be real and negative (so that $\eta_p > 0$ for $p \geq 1$); (iii) The eigenvectors should satisfy the orthonormality relation, Eq. (31). Instead of working with the asymmetric matrix $\mathscr{W}(s,s')$, for numerical purposes it is sometimes preferable to use the symmetric matrix $\mathscr{V}(s,s') = \mathscr{Z}(s)^{-1/2}\mathscr{W}(s,s')\mathscr{Z}(s')^{1/2}$, see Refs. [22, 23] for details. Indeed, the Matlab code we used to numerically solve the master equation, is based on the $\mathscr{V}$-matrix.

B. Survival and waiting time densities

In this section we derive the expression for the waiting and survival time densities given in Eqs. (22).

Denote by $\rho(t|s_{\rm init})$ the first passage time density starting from some initial position $s_{\rm init} \in \mathbb{R}1'$ or $\mathbb{R}0'$, see Fig. 5. The survival time density $\phi(t)$ and waiting time density $\psi(t)$ are then given by $\sum_{s_{\rm init}} \rho(t|s_{\rm init}) f(s_{\rm init})$, where $f(s_{\rm init})$ is the distribution of initial points $\in \mathbb{R}1'$ (for $\phi(t)$) or $\mathbb{R}0'$ (for $\psi(t)$). Following standard arguments (see, e.g, [26]) we can write the expression for $\rho(t|s_{\rm init})$,

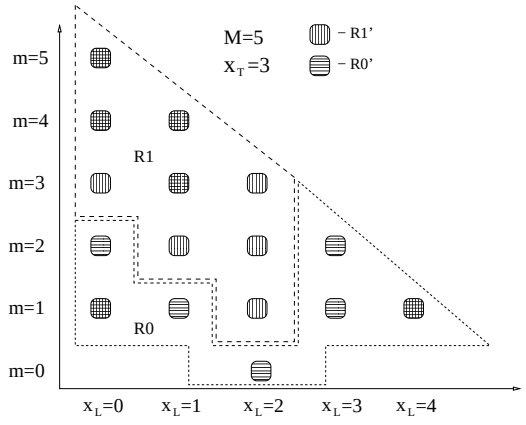


FIG. 5: Schematic of the (x_L, m)-points, region $\mathbb{R}1$ ($\mathbb{R}0$), for which the stochastic variable takes the value $I = 1$ ($I = 0$). The boundary points regions $\mathbb{R}1'$ and $\mathbb{R}0'$ are also indicated. The illustration is for the case $M = 5$ and $x_T = 3$, with $\Delta = 0$.

and therefore $\psi(t)$ and $\phi(t)$, which becomes:

$$\psi(t) = \sum_{p\in\mathbb{R}0} \bar{\eta}_p \bar{c}_p \exp(-\bar{\eta}_p t), \tag{32a}$$

$$\phi(t) = \sum_{p\in\mathbb{R}1} \bar{\eta}_p \bar{c}_p \exp(-\bar{\eta}_p t), \tag{32b}$$

where

$$\bar{c}_p = \sum_{s_{\rm init}} \frac{\bar{Q}_p(s_{\rm init}) f(s_{\rm init})}{P_{\rm eq}(s_{\rm init})} \sum_s \bar{Q}_p(s). \tag{33}$$

Here, $s \in \mathbb{R}0(\mathbb{R}1)$ for $\psi(t)$ ($\phi(t)$), and $\bar{\eta}_p$ and $\bar{Q}_p(s)$ are determined through the eigenvalue equation (21), which explicitly becomes in s-space [22]

$$\sum_{\tilde{s}} \mathscr{W}(s,\tilde{s}) \bar{Q}_p(\tilde{s}) = -\bar{\eta}_p \bar{Q}_p(s), \tag{34}$$

where $s, \tilde{s} \in \mathbb{R}1$ when calculating the survival time density, and $s, \tilde{s} \in \mathbb{R}0$ for the waiting time density.

The problem is now reduced to obtaining the distribution of initial points $f(s_{\rm init})$ such that agreement with the Gillespie time series (see Appendix A) is obtained for long times. We define the rate coefficients for jumps from the points in the boundary region $\mathbb{R}1$' to $\mathbb{R}0$' (see Figs. 3 and 5): $t_{1\to0}(s_{\rm init}) = t_L^+$, t_R^-, or t_G^-, where $s_{\rm init} \in \mathbb{R}1'$. Similarly, for jumps from the points in the boundary region $\mathbb{R}0$' to $\mathbb{R}1'$ ($s_{\rm init} \in \mathbb{R}0'$) we define: $t_{0\to1}(s_{\rm init}) = t_L^-$, t_R^+, or t_G^+. From the detailed balance condition we have that

$$\mathsf{t}_{1\to0}(s) P_{\rm eq}(s) = \mathsf{t}_{0\to1}(s') P_{\rm eq}(s'), \tag{35}$$

where s and s' are points in region $\mathbb{R}1$' and $\mathbb{R}0$' which are connected. For the the survival time density we then choose the distribution of initial points proportional to the stationary influx from region $\mathbb{R}0$'. Furthermore using the detailed balance condition and normalizing we have for the initial distribution in the $I = 1$ state

$$f(s_{\rm init}) = \frac{\mathsf{t}_{1\to0}(s_{\rm init}) P_{\rm eq}(s_{\rm init})}{\sum_{s_{\rm init}} \mathsf{t}_{1\to0}(s_{\rm init}) P_{\rm eq}(s_{\rm init})} \tag{36}$$

Similarly for the initial distribution in the I=0 state:

$$f(s_{\rm init}) = \frac{\mathsf{t}_{0\to1}(s_{\rm init}) P_{\rm eq}(s_{\rm init})}{\sum_{s_{\rm init}} \mathsf{t}_{0\to1}(s_{\rm init}) P_{\rm eq}(s_{\rm init})}, \tag{37}$$

which, together with Eqs. (32a), (32b) and (33), determines $\psi(t)$ and $\phi(t)$. We below proceed to show the choices above for $f(s_{\rm init})$ satisfy ergodicity requirements.

Ergodicity requires that the ratio of times spent in the I=1 and I=0 state equals

$$R_{\rm eq} = \frac{\sum_{s\in\mathbb{R}1} P_{\rm eq}(s)}{\sum_{s\in\mathbb{R}0} P_{\rm eq}(s)}. \tag{38}$$

From Eq. (32b) we have that the mean survival time can be written according to:

$$\tau_{\rm surv} = \int_0^\infty t\phi(t)dt = \sum_p (\bar{\eta}_p)^{-1} \bar{c}_p, \tag{39}$$

and identically for the mean waiting time $\tau_{\rm wait}$. We proceed by noticing that the eigenvalue equation (34) can be written as

$$\sum_{\tilde{s}} \left(\mathscr{W}^{\rm refl}(s,\tilde{s}) - \mathscr{W}^{\rm abs}(s,\tilde{s}) \right) \bar{Q}_p(\tilde{s}) = -\bar{\eta}_p \bar{Q}_p(s), \tag{40}$$

where

$$\mathscr{W}^{\rm abs}(s,\tilde{s}) = \mathsf{t}_{1\to0}(s) \delta_{s,\tilde{s}} \delta_{s,s_{\rm init}}, \tag{41}$$

with $s_{\rm init} \in \mathbb{R}1'$, and $\mathscr{W}^{\rm refl}(s,\tilde{s})$ satisfy $\sum_s \mathscr{W}^{\rm refl}(s,\tilde{s}) = 0$. Summing Eq. (34) over s and using the above identity we obtain

$$\sum_s \bar{Q}_p(s) = \sum_{s_{\rm init}} \bar{\eta}_p^{-1} \mathsf{t}_{1\to0}(s_{\rm init}) \bar{Q}_p(s_{\rm init}) \tag{42}$$

which is a useful connection between quantities in the bulk ($s \in \mathbb{R}1$) and at the boundary $s_{\rm init} \in \mathbb{R}1'$. Applying this relation to the expressions for the survival time, Eqs. (33), (36), and (39), we find

$$\tau_{\rm surv} = \frac{\sum_p \sum_s \sum_{\tilde{s}} \bar{Q}_p(s) \bar{Q}_p(\tilde{s})}{\sum_{s_{\rm init}} \mathsf{t}_{1\to0}(s_{\rm init}) P_{\rm eq}(s_{\rm init})}. \tag{43}$$

Finally, using the completeness relation [22]

$$\sum_p \frac{\bar{Q}_p(s) \bar{Q}_p(\tilde{s})}{P_{\rm eq}(\tilde{s})} = \delta_{s,\tilde{s}}, \tag{44}$$

we see that

$$\tau_{\rm surv} = \frac{\sum_{s\in\mathbb{R}1} P_{\rm eq}(s)}{\sum_{s_{\rm init}} \mathsf{t}_{1\to0}(s) P_{\rm eq}(s_{\rm init})}. \tag{45}$$

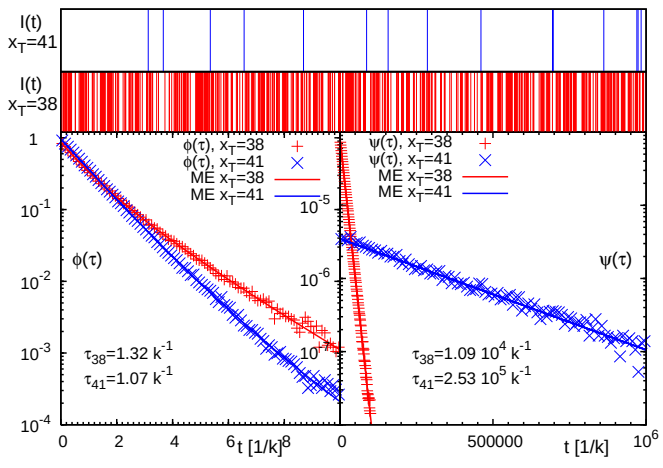


FIG. 6: Top: Fluorescence time series $I(t)$ for the T7 promoter sequence, with tag position $x_T = 38$ (red) and $x_T = 41$ (blue). Bottom: Waiting time ($\psi(\tau)$) and fluorescence survival time ($\phi(\tau)$) densities, in units of k. The data points (solid lines) are results from the Gillespie algorithm (master equation). All results are for $T = 37°C$ and 100 mM NaCl with DNA parameters from [8].

In a similar fashion

$$\tau_{\rm wait} = \frac{\sum_{s\in\mathbb{R}0} P_{\rm eq}(s)}{\sum_{s_{\rm init}} \mathsf{t}_{0\to 1}(s) P_{\rm eq}(s_{\rm init})}, \tag{46}$$

which, using the detailed balance condition, Eq. (35), shows that $\tau_{\rm surv}/\tau_{\rm wait} = R_{\rm eq}$.

With the completeness relation (44) and Eq. (42) we find from Eqs. (33), (36), and (37) that $\bar{c}_p$ can be written

$$\bar{c}_p = \frac{\bar{\eta}_p[\sum_s \bar{Q}_p(s)]^2}{\sum_p \bar{\eta}_p[\sum_s \bar{Q}_p(s)]^2} \tag{47}$$

which is the form given in Eq. (22c).

We show in Fig. 6 the time series obtained from a stochastic simulation (see Appendix A for a short introduction, and refer to Ref. [27] for details) for two different tag positions in the T7 bacteriovirus promoter sequence

```
     1                   20
     |                   |
5'-aTGACCAGTTGAAGGACTGGAAGTAATACGACTC
   AGTATAGGGACAATGCTTAAGGTCGCTCTCTAGGAg-3'
      |  |                           |
     38 41                          68
```
(48)

whose TATA motif is marked in red [28]. A promoter is a sequence (often containing the so called TATA motif) marking the start of a gene, to which RNA polymerase is recruited and where transcription then initiates. Fig. 6 shows the signal $I(t)$ at 37°C for the tag positions $x_T = 38$ in the core of TATA, and $x_T = 41$ at the second GC bp after TATA. Bubble events occur much more frequently in TATA (the TA/AT stacking interaction is particularly weak [8]). This is quantified by the density of waiting times $\psi(\tau)$ spent in the $I = 0$ state, whose characteristic time scale $\tau' = \int_0^\infty d\tau\tau\psi(\tau)$ is more than an order of magnitude longer than at $x_T = 41$. In contrast, we observe similar behavior for the density of opening times $\phi(\tau)$ for $x_T = 38$ and 41. The solid lines are the results from the master equation, see subsection III B, showing excellent agreement with the Gillespie results. Notice that whereas $\psi(t)$ is characterized by a single exponential, $\phi(t)$ show a crossover between different regimes. For long times both $\psi(\tau)$ and $\phi(\tau)$ decay exponentially as it should for a finite DNA stretch.

V. REDUCED ONE-VARIABLE SCHEME FOR A HOMOPOLYMER

After addressing the derivation of the probability densities $\psi(t)$ and $\phi(t)$, and the details concerning the transfer matrix $\mathscr{W}$, we show how the master equation formalism reduces when a homopolymer sequence is considered, that is, a sequence with only one type of bps such as $(AT)_N$. Homopolymers can be realized experimentally. In the case they are clamped, possible secondary structure formation does not appear to occur, and our formalism remains valid. In the case of long homopolymers, imperfect matching conditions apply, and additional degrees of freedom emerge [2]. Although this can be straightforwardly included in the formalism, we do not consider this case here.

In the homopolymer case, it is possible to obtain analytical results. To that end we note that for a homopolymer, all bps have the same statistical weights $u_{\rm st}(x)$ and $u_{\rm hb}(x)$. Formally, we therefore use $u = u_{\rm st}u_{\rm hb}$ for disruption of additional bps after bubble initiation. Due to this choice, we need to utilize the initiation factor σ_0 instead of the ring factor ξ, as σ_0 takes care of the fact that upon initiation two stacking bonds are broken [6, 8, 29]. If we furthermore assume that we are below the melting temperature $u < 1$, have a long DNA region $M \gg 1$ and consider bubbles far from the clamping, end effects are much less pronounced. It then follows that $P(x_L, m, t; x_L', m') = \tilde{P}(m, t; m')$, and the master equation reduces to

$$\begin{aligned}\frac{\partial}{\partial t}\tilde{P}(m,t) &= \tilde{\mathsf{t}}^+(m-1)\tilde{P}(m-1,t) \\ &\quad +\tilde{\mathsf{t}}^-(m+1)\tilde{P}(m+1,t) \\ &\quad -(\tilde{\mathsf{t}}^+(m)+\tilde{\mathsf{t}}^-(m))\tilde{P}(m,t),\end{aligned} \tag{49}$$

with the short-hand notation $\tilde{P}(m,t) = \tilde{P}(m,t;m')$. The forward transfer coefficients in this limit are given by

$$\begin{aligned}\tilde{\mathsf{t}}^+(m=0) &= k\sigma_0 u s(0) \\ \tilde{\mathsf{t}}^+(m)|_{m\geq 1} &= kus(m),\end{aligned} \tag{50}$$

where we have incorporated the fact that a bubble size increase can occur by opening of a bp at either the left or the right fork. For the backward transfer coefficients,

we find

$$\tilde{\mathsf{t}}^{-}(m) = k. \tag{51}$$

The eigenvalue equation corresponding to Eq. (49) has the comparatively simple structure

$$\begin{aligned}&\tilde{\mathsf{t}}^{+}(m-1)\tilde{Q}_p(m-1)\\ &+\tilde{\mathsf{t}}^{-}(m+1)\tilde{Q}_p(m+1)\\ &-(\tilde{\mathsf{t}}^{+}(m)+\tilde{\mathsf{t}}^{-}(m))\tilde{Q}_p(m) = -\tilde{\eta}_p\tilde{Q}_p(m),\end{aligned} \tag{52}$$

with eigenvalues $\tilde{\eta}_p$ and eigenvectors $\tilde{Q}_p(m)$ ($p = 0, 1, \ldots, M$). The equation above is identical to the one in [16, 24], and thus our generalized formalism is consistent with previous homopolymer models [16, 24]. We note that the equilibrium distribution becomes

$$\tilde{P}_{\rm eq}(m) = \frac{\mathscr{Z}(m)}{\sum_{m=0}^{M}\mathscr{Z}(m)}, \tag{53}$$

where $\mathscr{Z}(m) = \sigma_0(1+m)^{-c}u^m$ with $\mathscr{Z}(0) = 1$, see Eqs. (1) and (2).

The autocorrelation function is, as before, simply proportional to the joint probability of having $m \geq 1$ at time t and $m \geq 1$ at initial time $t = 0$. Proceeding as previously, and assuming that initially the system is at equilibrium, $P(m, 0; m', 0) = \delta_{mm'}\tilde{P}_{\rm eq}(m)$, we have

$$\tilde{A}(t) = \langle I(t)I(0)\rangle - (\langle I\rangle)^2 = \sum_{p\neq 0}\left(\tilde{T}_p\right)^2 \exp\left(-\frac{t}{\tilde{\tau}_p}\right), \tag{54}$$

where $\tilde{T}_p = \sum_{m=1}^{M}\tilde{Q}_p(m)$. Here, we introduced the relaxation times $\tilde{\tau}_p \equiv 1/\tilde{\eta}_p$. As before, we write the correlation function according to $\tilde{A}(t) = \int d\tau \exp(-t/\tau)\tilde{f}(\tau)$, with the relaxation time spectrum

$$\tilde{f}(\tau) = \sum_{p\neq 0}\left(\tilde{T}_p\right)^2 \delta(\tau - \tilde{\tau}_p). \tag{55}$$

In Fig. 7, we compare the approximate result for $A(x_T, t)$ obtained by numerical solution of Eqs. (52), and using Eq. (54), with the general result from the master equation in Section III. We also show the corresponding weighted spectral densities given by Eq. (55). We note that the approximate expression works well only for the case of internal tagging and temperatures below the melting temperature (and for a sufficiently long DNA region); for a short DNA sequence, close-to-end-tagging or high temperatures (i.e., large bubbles) end effects, which are not included in the approximate model above, are significant.

In the analysis of Refs. [17, 24] it was found that close to the melting transition at T_m, the mean correlation function takes its maximum (critical slowing down). In order to get an understanding of this behavior we here analytically obtain the largest relaxation time from the homopolymer model above. From Reference [15] we have that the eigenvalues, see Eq. (52), are for $c = 0$

$$\tilde{\eta}_p = k(u + 1 - 2u^{1/2}\cos\omega_p) \tag{56}$$

where ω_p ($0 < \omega_p \leq \pi$) is obtained from the transcendental equation

$$g(\omega_p) = \sin[(M+1)\omega_p] - \delta\sin[M\omega_p] = 0 \tag{57}$$

with $\delta = (1-\sigma_0)u^{1/2}$. For $u \to 1$ and $\sigma_0 \to 0$ we get

$$\begin{aligned}g(\omega_p) &= \sin[(M+1)\omega_p] - \sin[M\omega_p]\\ &= 2\sin\frac{\omega_p}{2}\cos[(M+\frac{1}{2})\omega_p]\end{aligned} \tag{58}$$

so that we have

$$\omega_p = \frac{(p-1/2)\pi}{M+1/2} \tag{59}$$

which together with Eq. (56) give the eigenvalues. The smallest eigenvalue (largest relaxation time) is obtained for $p = 1$, i.e. $\tilde{\eta}_1 = 2k(1-\cos(\pi/[2M+1])) \approx k\pi^2/(2M+1)^2$ for $M \gg 1$, and therefore the largest relaxation time becomes

$$\tilde{\tau}_1 = \frac{1}{\tilde{\eta}_1} \approx \frac{(2M+1)^2}{\pi^2}k^{-1} \tag{60}$$

We notice that the longest relaxation time scales as $\sim M^2$ at melting, in agreement with the findings in [30]. Fig. 8 demonstrates the good agreement of the homopolymer result ($\tau_{\max}$, 1D in the figure) with the maxima of the correlation time, that coincide with the melting concentration.

VI. CONCLUSIONS

In this study we considered the bubble breathing dynamics in a heteropolymer DNA-region characterized by statistical weights $u_{\rm st}(x)$ for disrupting a stacking interaction between neighboring bps, and the weight $u_{\rm hb}(x)$ for breaking a Watson-Crick hydrogen bond (x labels different bps), as well the bubble initiation parameter (the ring-factor) σ_0 (ξ). For that purpose, we introduced a $(2+1)$-variable master equation governing the time evolution of the probability distribution to find a bubble of size m with left fork position x_L at time t, as well as a complementary Gillespie scheme. The time averages from the stochastic simulation agree well with the ensemble properties derived from the ME. We calculate the spectrum of relaxation times, and in particular the experimentally measurable autocorrelation function of a tagged bp is obtained. All parameters in our model are known from recent equilibrium measurements available for a wide range of temperatures and NaCl concentrations, except for the rate constant k for (un)zipping that is the only free fit parameter. A better understanding of the zipping rate k remains an open question, requiring a detailed microscopic modelling of DNA-breathing.

For the case of a long homopolymer DNA region with internal tagging and below the melting temperature the position of the bubble becomes negligible, and the master equation reduces to previous (1+1)-variable approaches in terms of the bubble size.

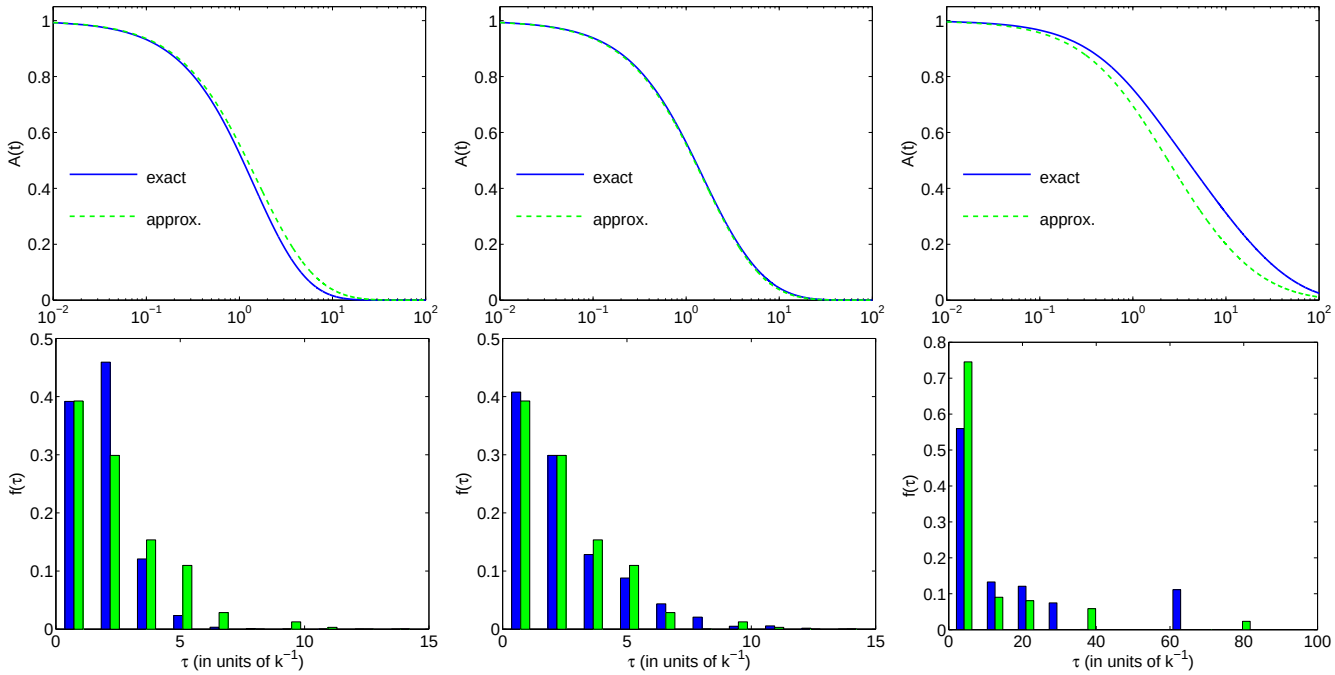


FIG. 7: Autocorrelation $A(t)$ and spectral density $f(\tau)$ for a tagged bp in a homopolymer region: $u = u_{\rm hb}u_{\rm st}$. Left: Close-to-end-tagging far from T_m ($x_T = 2$, $u = 0.6$). Middle: Center-tagging far from T_m ($x_T = 20$, $u = 0.6$). Right: Center-tagging close to T_m ($x_T = 20$, $u = 0.9$). In the $A(t)$ plots the blue curves are the exact result. The dashed green curves are approximated from from Eqs. (52) and (54). In the spectral density plot the data were collected into 10 bins. The green bars are the approximate one-variable results, Eq. (55), and the blue bars are the exact result. The length of the DNA segment was $M = 40$. The approximate expression only works well for internal tagging and below T_m.

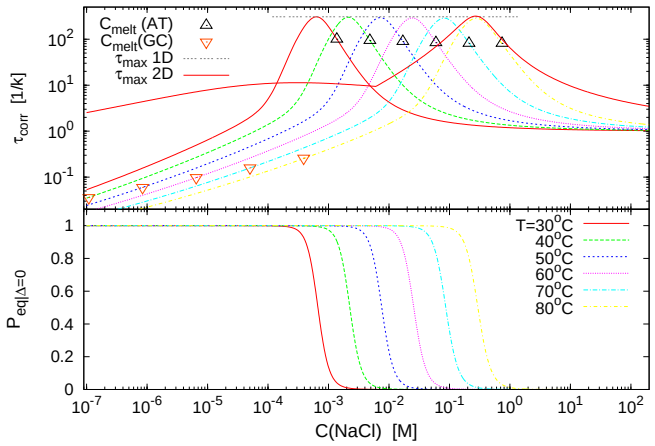


FIG. 8: Top: Mean correlation time $\tau_{\rm corr} = \int_0^\infty dt' A(t')/A(0)$ versus NaCl concentration for various temperatures T for the AT9 construct of Ref. [11], showing a critical slowing down at the melting concentration (compare lower panel). The triangles denotes the melting concentration for infinitely long random AT and GC stretches. The curve denoted by $\tau_{\rm max1D}$ is the result given in Eq. (60), and $\tau_{\rm max2D} = \max\{\tau_p\}$, $p = 1, \ldots, S$ is the maximum relaxation time of the full problem specified in Sec. III. Bottom: Opening probability of bp x_T.

Acknowledgments

We thank Maxim Frank-Kamenetskii, Oleg Krichevsky, and Kim Splitorff for very helpful discussion. SKB acknowledges support from Virginia Tech through ASPIRES award program. TA acknowledges partial support through a Research Career Award from the Knut and Alice Wallenberg foundation. RM acknowledges partial funding from the Natural Sciences and Engineering Research Council (NSERC) of Canada and the Canada Research Chairs program.

APPENDIX A: GILLESPIE APPROACH

In this section we briefly review the Gillespie algorithm. Together with the explicit expressions for the transfer coefficients introduced in the previous section it is used to generate stochastic time series of bubble breathing. In particular we show how the motion of a tagged bp is obtained.

To denote a bubble state of m broken bps at position x_L we define the occupation number $b(x_L, m)$ for each lattice point in Fig. 3 with the properties $b(x_L, m) = 1$ if the particular state $\{x_L, m\}$ is occupied and $b(x_L, m) = 0$ for unoccupied states. For the completely zipped state $m = 0$ there is no dependence on x_L, and we intro-

duce the occupation number $b(0)$. The stochastic DNA breathing then corresponds to the nearest neighbor jump processes in the triangular lattice in Fig. 3. Each jump away from the state $\{x_L, m\}$ (i.e., from the state with $b(x_L, m) = 1$) occurs at a random time τ and in a random direction to one of the nearest neighbors; it is governed by the reaction probability density function [31, 32]

$$P(\tau, \mu, \nu) = \mathsf{t}^{\mu}_{\nu}(x_L, m) \exp\left(-\tau \sum_{\mu,\nu} \mathsf{t}^{\mu}_{\nu}(x_L, m)\right), \quad \text{(A1)}$$

which for a given state (x_L, m) defines after what waiting time τ the next step occurs and in what 'direction', $\nu \in \{G, L, R\}$, $\mu \in \{+/-\}$. A simulation run produces a time series of occupied states $\{x_L, m\}$ and how long time $\tau = \tau_j$ ($j = 1, ..., N$, where N is the number of steps in the simulation) this particular state is occupied. This waiting time τ, that is, according to Eq. (A1) follows a Poisson distribution [33].

1. Tagged bp survival and waiting time densities

The stochastic variable $I(t)$ is then obtained by summing the Gillespie occupation number $b(x_L, m)$ ($b(x_L, m)$ takes only values 0 or 1) over region $\mathbb{R}1$, i.e.

$$I(t) = \sum_{x_L, m \in \mathbb{R}1} b(x_L, m). \quad \text{(A2)}$$

From the time series for $I(t)$ one can, for instance, calculate the waiting time distribution $\psi(\tau)$ of times spent in the $I = 0$ state, as well as the survival time distribution $\phi(\tau)$ of times in the $I = 1$ state. Explicit examples for $\psi(\tau)$ and $\phi(\tau)$ are shown in Sec. IV.

The probability that the tagged bp is open becomes

$$P_G(t_j) = \frac{1}{t_N} \sum_{j=1}^{N} \tau_j I(t_j) \quad \text{(A3)}$$

where $t_j = \sum_{j'=1}^{j} \tau_{j'}$. For long times the explicit construction of the Gillespie scheme together with the detailed balance conditions guarantee that $P_G(t_j)$ tends to the equilibrium probability, i.e. that $P_G(t_j \to \infty) = \sum_{x_L, m \in \mathbb{R}1} P^{\rm eq}(x_L, m)$, where $P^{\rm eq}(x_L, m)$ is given in Eq. (2).

2. Tagged base-pair autocorrelation function

The autocorrelation function for a tagged bp is obtained through

$$\begin{aligned} A_t(x_T, t) &= \overline{I(t)I(0)} - (\overline{I(t)})^2 \\ &= \frac{1}{T}\int_0^T I(t+t')I(t')dt' - \left(\frac{1}{T}\int_0^T I(t')dt'\right)^2 \quad \text{(A4)} \end{aligned}$$

which for long times agrees with the the ensemble average, Eq. (14), from the master equation. The function $A_t(x_T, t)$ corresponds to the blinking autocorrelation function obtained in the FCS experiment from Ref. [11].

[1] A. Kornberg, DNA Synthesis (W. H. Freeman, San Francisco, CA, 1974).
[2] D. Poland and H. A. Scheraga, Theory of Helix-Coil Transitions in Biopolymers (Academic Press, New York, 1970).
[3] R. M. Wartell and A. S. Benight, Phys. Rep. **126**, 67 (1985).
[4] C. R. Cantor and P. R. Schimmel, Biophysical Chemistry, Part 3 (W. H. Freeman, New York, 1980).
[5] Note that for $T = 37°$C we used that $1k_BT = 0.62$kcal/mol. Also note that writing Boltzmann factors for the free energies as $\exp(\beta\Delta G)$, with $\beta = 1/(k_BT)$, a positive ΔG denotes an unstable bond.
[6] R. D. Blake, J. W. Bizzaro, J. D. Blake, G. R. Day, S. G. Delcourt, J. Knowles, K. A. Marx, and J. SantaLucia Jr., Bioinformatics **15**, 370 (1999).
[7] R. Blossey and E. Carlon, Phys. Rev. E **68**, 061911 (2003).
[8] A. Krueger, E. Protozanova, and M. D. Frank-Kamenetskii, Biophys. J. **90**, 3091 (2006).
[9] E. Protozanova, P. Yakovchuk, and M. D. Frank-Kamenetskii, J. Mol. Biol. **342**, 775 (2004).
[10] M. Guéron, M. Kochoyan, and J.-L. Leroy, Nature **328**, 89 (1987).
[11] G. Altan-Bonnet, A. Libchaber, and O. Krichevsky, Phys. Rev. Lett. **90**, 138101 (2003).
[12] K. Pant, R. L. Karpel, and M. C. Williams, J. Mol. Biol. **327**, 571 (2003).
[13] K. Pant, R. L. Karpel, I. Rouzina, and M. C. Williams, J. Mol. Biol. **336**, 851 (2004).
[14] R. L. Karpel, IUBMB Life **53**, 161 (2002).
[15] T. Ambjörnsson and R. Metzler, Phys. Rev. E **72**, 030901(R) (2005).
[16] T. Ambjörnsson and R. Metzler, J. Phys. Cond. Mat. **17**, S1841 (2005).
[17] T. Ambjörnsson, S. K. Banik, and R. Metzler, Biophys. J., submitted.
[18] M. Fixman and J. J. Freire, Biopol. **16**, 2693 (1977).
[19] See C. Richard and A. J. Guttmann, J. Stat. Phys. **115**, 925 (2004) and Refs. therein.
[20] H. Risken, The Fokker-Planck equation (Springer-Verlag, Berlin, 1989).
[21] Also, $\mathsf{t}^{+}_{L}(x_L = -1, m) = 0$ and $\mathsf{t}^{-}_{R}(x_L, m = M - x_L + 1) = 0$ for $m = 2, ..., M + 1$ for completeness.
[22] N. G. van Kampen, Stochastic Processes in Physics and Chemistry, 2nd Ed. (North-Holland, Amsterdam, 1992).
[23] C. W. Gardiner, Handbook of Stochastic Methods for Physics, Chemistry and the Natural Sciences (Springer,

Berlin, 1989).
[24] T. Ambjörnsson, S. K. Banik, and R. Metzler, Phys. Rev. Lett. **97**, 128105 (2006).
[25] E. A. Di Marzio, C. M. Guttman, and J. D. Hoffman, Faraday Disc. **68**, 210 (1979).
[26] T. Ambjörnsson, M. A. Lomholt, and R. Metzler, J. Phys. Cond. Mat. **17**, S3945 (2005).
[27] S. K. Banik, T. Ambjörnsson, and R. Metzler, Europhys. Lett. **71**, 852 (2005).
[28] G. Kalosakas, K. Ø. Rasmussen, A. R. Bishop, C. H. Choi, and A. Usheva, Europhys. Lett. **68**, 127 (2004).
[29] J. SantaLucia Jr., Proc. Natl. Acad. Sci. USA **95**, 1460 (1998).
[30] D. J. Bicout and E. Kats, Phys. Rev. E **70**, 010902(R) (2004).
[31] D. T. Gillespie, J. Comp. Phys. **22**, 403 (1976).
[32] D. T. Gillespie, J. Phys. Chem. **81** 2340 (1977).
[33] D. R. Cox, Renewal Theory (J. Wiley & Sons, New York, NY, 1962).